

**Keywords:** biliverdin; HNSCC, head and neck squamous cell carcinoma; ROS, reactive oxygen species; EGFR; proliferation

# Biliverdin's regulation of reactive oxygen species signalling leads to potent inhibition of proliferative and angiogenic pathways in head and neck cancer

J Zheng<sup>1,2</sup>, D A Nagda<sup>1</sup>, S A Lajud<sup>1</sup>, S Kumar<sup>1</sup>, A Mouchli<sup>1</sup>, O Bezpalko<sup>1</sup>, B W O'Malley Jr<sup>1</sup> and D Li<sup>\*1</sup>

<sup>1</sup>Department of Otorhinolaryngology—Head and Neck Surgery, University of Pennsylvania Perelman School of Medicine, 415 Curie Boulevard, Clinical Research Building, Philadelphia, PA, USA and <sup>2</sup>Department of Oral and Maxillofacial Surgery, Hospital of Stomatology, Xi'an Jiaotong University, Xi'an, Shaanxi, China

**Background:** In this study, we evaluate whether the use of biliverdin (BV), a natural non-toxic antioxidant product of haeme catabolism, can suppress head and neck squamous cell carcinoma (HNSCC) cell proliferation and improve the tumour survival both *in vitro* and *in vivo*. Furthermore, we investigate whether this therapeutic outcome relies on BV's potent antioxidant effect on reactive oxygen species (ROS)-mediated signalling.

**Methods:** Two well-characterised HNSCC cell lines and a mouse model with human HNSCC were used for this study. *In vitro*, the effect of BV on ROS was assayed. Subsequently, critical regulatory proteins involved in growth, antiapoptotic, and angiogenic pathways were investigated by western blot analysis. In addition, the antiproliferative effect of BV was also evaluated using the clonogenic assay. Moreover, tumour growth inhibition was assessed using a mouse model with HNSCC.

**Results:** Biliverdin treatment resulted in decreased ROS, leading to suppression of proliferation and angiogenesis pathways of HNSCC, significantly decreasing the expression and phosphorylation of oncogenic factors such as epidermal growth factor receptor (EGFR), phosphorylation of Akt, and expression of angiogenic marker and transcription factor, hypoxia-inducible factor1- $\alpha$  (HIF1- $\alpha$ ). Furthermore, this downregulation of ROS by BV led to a significant suppression of tumour growth *in vivo*.

**Conclusions:** Our study demonstrates the efficacy of a novel therapeutic approach using BV as an antitumour agent against HNSCC through its effect on EGFR/Akt and HIF1- $\alpha$ /angiogenesis signal transduction pathways. Our findings indicate that BV's inhibitory effect on these tumorigenic pathways relies on its antioxidant effect, and may extend its therapeutic potential to other solid cancers.

Head and neck cancer (HNC) is the sixth most common cancer worldwide, accounting for over 350 000 deaths annually. In the United States alone, more than 50 000 patients were diagnosed with HNC in 2012 (Leemans *et al*, 2011). Approximately 90% of all HNCs are squamous in origin, commonly referred to as head and neck squamous cell carcinoma (HNSCC), and originate from the epithelial lining of the upper aerodigestive tract. Despite several advances in treatment options, 3-year disease-free survival still ranges around 35–55%, and has hardly improved over the past 30

years (Li *et al*, 2008). In addition, current therapeutic modalities such as chemotherapy and radiation are marked by high toxicity, poor treatment-related side effects, and acquired resistance. There is, therefore, a great need for the development of novel 'chemoradiation-free' therapies to target key molecular pathways in HNSCC cells while preserving normal surrounding tissue.

Biliverdin (BV) is a natural, non-toxic, antioxidant green tetrapyrrole bile pigment, and is a product of the haeme catabolic pathway (Mosqueda *et al*, 2005). While initially BV was viewed as a

\*Correspondence: Dr D Li; E-mail: lidaqing@mail.med.upenn.edu

Received 5 July 2013; revised 29 January 2014; accepted 30 January 2014; published online 25 February 2014

© 2014 Cancer Research UK. All rights reserved 0007–0920/14

mere waste product excreted in bile, recent studies have elucidated its beneficial effects (Liu *et al*, 2003; Fondevila *et al*, 2004; Yamashita *et al*, 2004; Sarady-Andrews *et al*, 2005), such as its ability to regulate cellular growth in hyperproliferative disorders. Specifically, BV and its rapidly converted homologue bilirubin (BR) have been shown to slow growth of cells involved in several pathological processes, such as intimal growth after blood vessel injury and cancer propagation (Ollinger *et al*, 2005, 2007b). In addition, a negative correlation between serum BR levels and cancer incidence was established through multiple clinical studies (Temme *et al*, 2001; Ching *et al*, 2002; Zucker *et al*, 2004). Furthermore, in both *in vitro* and *in vivo* models, BR was shown to significantly downregulate cancer cell growth, but the primary mechanism governing the role of BR-induced cellular growth inhibition was largely undetermined. Additionally, BR is highly toxic to normal cells, relies on carrier-mediated transport in the blood, and its mechanism of entry into cells is not well understood.

Head and neck squamous cell carcinoma commonly over-expresses several growth factors and their receptors, including epidermal growth factor receptor (EGFR), a cell-surface receptor tyrosine kinase, which has been associated with poor prognosis and decreased survival. One important downstream target of EGFR is Akt, a serine/threonine kinase (Dudek *et al*, 1997), which has been shown to be a critical transmitter of oncogenic signalling in tumours (Dobashi *et al*, 2011). After EGFR activation, Akt is recruited to the plasma membrane by PIP3, and then phosphorylated at Thr308 by protein-dependent kinase 1 (PDK1). For full activation, Akt needs to be subsequently phosphorylated at Ser473 by PDK2. On the basis of the finding that BR blocked vascular smooth muscle cell development and cancer cell proliferation (Ollinger *et al*, 2005, 2007a), we looked to evaluate whether BV, a non-toxic homologue of BR, could exhibit a potent antiproliferative effect on HNSCC cells. Moreover, we investigated whether this inhibitory effect of BV could be translated to an *in vivo* mouse model. Furthermore, we look to elucidate the mechanism underlying these findings, and evaluate whether the pathway relies on EGFR deprivation, leading to a subsequent downregulation of proliferative and antiapoptotic pathways.

Previously, BV has been shown to possess highly potent antioxidant properties; significantly more so than BR or other tetrapyrroles found in the body (Asad *et al*, 2001; Stocker, 2004; MacLean *et al*, 2008; Molzer *et al*, 2012). Furthermore, reactive oxygen species (ROS)-mediated cellular signalling has shown to be critical for cellular growth, angiogenic, and other oncogenic pathways. Specifically, increased oxidative stress in cancer cells leads to upregulation of hypoxia-inducible factor1- $\alpha$  (HIF1- $\alpha$ ) (Ahluwalia and Tarnawski, 2012), a critical player in angiogenesis, which leads to increased VEGF production from the cells, among

several other pro-angiogenic factors (Choi *et al*, 2003). Therefore, in this study we investigate the effect of BV on ROS in HNSCC cells, and whether this effect leads to a downregulation of HIF1- $\alpha$  *in vitro* and angiogenesis *in vivo*.

## MATERIALS AND METHODS

**Cell culture.** Previously well-characterised human HNSCC cell lines Fadu and JHU022 originating from primary tumour explants (Li *et al*, 2008) and human umbilical vein endothelial cells (HUVECs) were used in this study. Cells were propagated in RPMI-1640 with 10% FBS, 1% Penicillin, and 1% Streptomycin (HUVECs were propagated in endothelial cell growth media kit, cc-4133; Lonza, Allendale, NJ, USA) at 37 °C with 5% CO<sub>2</sub>.

**Reagents.** For *in vitro* experiments, BV (Frontier Scientific, Logan, UT, USA) was first dissolved in 0.1% DMSO (Sigma-Aldrich, St Louis, MO, USA) and then adjusted to an appropriate final concentration using prewarmed culture medium as described by Dortay *et al* (2011). In all *in vitro* experiments where BV was used, the corresponding amount of DMSO was added to the medium to ensure appropriate control conditions. For *in vivo* study, BV was dissolved in PBS and neutralised with 1 N HCl to a pH of 7.4, and a final concentration of 1 mM. Subsequently, the solution was sterilised by filtration and stored at -80 °C. All experiments were carried out in a controlled manner to avoid direct light exposure. 5,5'-Dithio-bis-(2-nitrobenzoic acid), (DTNB) was purchased from Thermo Scientific (Rockford, IL, USA). 6-hydroxy-2,5,7,8-tetramethylchroman-2-carboxylic acid (Trolox) was purchased from Cayman chemical (Ann Arbor, MI, USA). Barium chloride dihydrate and benzene were purchased from Sigma-Aldrich. Matrigel was purchased from BD Biosciences (San Jose, CA, USA).

***In vitro* clonogenic assay.** Cell proliferation was evaluated using the clonogenic assay. Cells were plated at 400 cells per well in a 6-well plate and were treated as indicated. Seventy-two hours after treatment, growth medium was changed and cells were cultured at 37 °C for 7 days. Cells were washed once with PBS, stained with crystal violet (Bio-Rad, Hercules, CA, USA) for 30 min at room temperature. Colonies per well were enumerated, and the mean  $\pm$  s.d. was determined. The survival fraction was calculated and expressed as compared with control. All groups were tested in three independent experiments.

**Measurement of intracellular ROS.** Seventy-two hours after treatment with 100  $\mu$ M BV, cells were added the CellROX Reagent (Carlsbad, CA, USA) at a final concentration of 5  $\mu$ M. The cells were then incubated for 30 min at 37 °C. The cell-culture

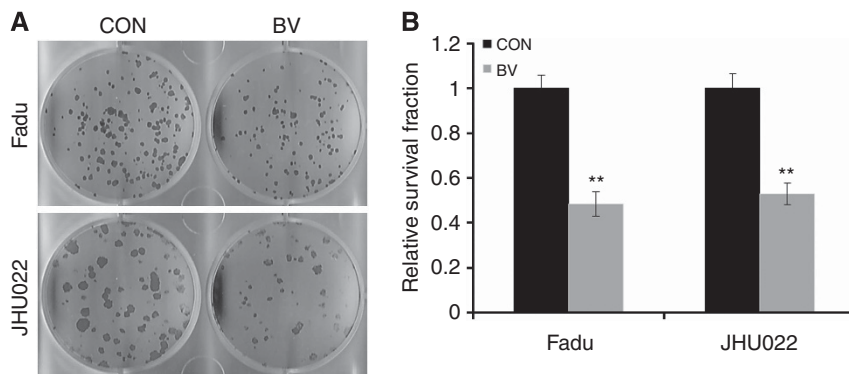


**Figure 1.** BV suppresses HNSCC cell colony formation *in vitro*. To demonstrate the antiproliferative effect of BV, a clonogenic assay was performed on Fadu (A) and JHU022 (B) cancer cells as described earlier. In three independent experiments with at least six samples each, treatment with BV significantly suppressed the colony formation ability of all two HNSCC cells tested (\*\* $P < 0.01$ ). Survival fraction  $\pm$  s.d. is shown.

supernatant was removed and cells were washed with PBS for three times, and the fluorescence intensity was obtained with an Infinite M1000 multimode reader (TECAN, San Jose, CA, USA).

**Western blot analysis.** Antibodies used for western blot analysis were anti-EGFR, anti-phosphorylated EGFR (p-EGFR) (Cell Signaling, Boston, MA, USA), anti-Akt, anti-phosphorylated Akt (p-Akt) (Novus Biologicals, Littleton, CO, USA), anti-PARP (GeneTex, Irvine, CA, USA; Abcam, Cambridge, MA, USA), anti-HIF1- $\alpha$  (Cell Signaling), anti-phosphorylated-Rb (Cell Signaling), anti-Cyclin D1 (BD Biosciences), and anti  $\beta$ -actin (Novus Biologicals). To analyse the effects of BV on these proteins, Fadu and JHU022 cells were seeded at 300 000 cells per well in a 6-well plate, treated as described in the legend, and protein samples were collected at 72 h. Cells were then lysed with lysis buffer (150 mM sodium chloride, 1.0% NP-40, 0.5% sodium deoxycholate, 0.1% SDS, and 50 mM Tris, pH 8.0, protease inhibitor cocktail, and phosphatase inhibitor cocktail tablets) and protein concentration was determined using BCA (Pierce, Rockford, IL, USA). Western blot analysis was then conducted, with  $\beta$ -actin serving as a loading control.

**Immunohistochemistry.** Immunohistochemistry (IHC) was performed using the VECTASTAINVR Elite ABC kit (Vector Laboratories, Inc., Burlingame, CA, USA) to visualise endothelial cells (CD31, platelet/endothelial cell adhesion molecule-1) in tumour samples. Formalin-fixed paraffin-embedded tumour tissue sections were cut at 5  $\mu$ m thick and air dried for 4 h. Sections were then incubated with normal blocking serum for 20 min at room temperature, followed by the primary antibody at 4 °C overnight in the dark. Rat monoclonal antibody to mouse CD31 antigen (BD Pharmingen, San Diego, CA, USA) was used at a dilution of 1 : 50. Sections were incubated with diluted biotinylated secondary antibody solutions, followed by VECTASTAINVR Elite ABC reagent for 30 min. Subsequently, sections were incubated with 3,3'-diaminobenzidine tetrahydrochloride (DAB)-H<sub>2</sub>O<sub>2</sub> solution for visualisation and were counterstained with haematoxylin. To assess the grade of microvessel growth within the tumour, three views ( $\times 20$ ) were digitally recorded for each tumour to cover the greatest anti-CD31 staining area for estimation of microvessel development (Mavria *et al*, 2005; Saito *et al*, 2009). The relative percentage of CD31-positive area, represented by the microvessel density (MVD) within each high power field, was measured for three separate images with the assistance of ImmunoRatio, an application reviewed in detail by Tuominen *et al* (2010).

**Matrigel tube formation assay.** Tube formation assay was performed by following the published protocol by Arnaoutova *et al* (2009). Briefly, 8-well chamber slides were coated with ice-cold Matrigel (BD Biosciences) (150  $\mu$ l per well) and incubated at 37 °C for 30 min to allow gelation to occur. Human umbilical vein endothelial cells treated with BV (100  $\mu$ M) or Trolox (1 mM), known as an antioxidant, or DTNB or BV plus DTNB, were incubated in endothelial cell growth media for 3 days. After the treatment, HUVECs were added to the top of the gel at a density of 50 000 cells per well. The positive control included the same amount of solvation vehicle (DMSO) as the experimental condition. Cells were incubated at 37 °C with 5% CO<sub>2</sub> for 24 h and images were captured with a SPOT CCD camera mounted on Nikon Eclipse 80i fluorescence microscope (Nikon, Melville, NY, USA).

**Plasma alanine transaminase assay.** The levels of nude mouse plasma alanine transaminase (ALT) were measured and calculated using the Cayman's Alanine Transaminase Assay Kit (Ann Arbor, MI, USA) by following the kit protocol. The plasma was collected from three BALB/c nude mice in each group with or without giving 12 days BV intraperitoneal (i.p.) injection. Porcine heart ALT was used as a positive control (kit provided).

**BR level measurement *in vitro*.** Fadu and JHU022 cells were treated with or without 5  $\mu$ M DTNB, 100  $\mu$ M BV, or 100  $\mu$ M BV plus 5  $\mu$ M DTNB for 3 days. Then, the culture supernatant was collected and measured the BR level by using the protocol which has been reported by Dhouib *et al* (Turcanu *et al*, 1998).

**Apoptosis detection.** Apoptosis was quantified in tumour samples using the Apoptosis Detection Kit (Millipore, Billerica, MA, USA). Tumour samples were fixed in formalin and embedded in paraffin as per previously established protocols. Tissue samples were sectioned at 5  $\mu$ m thickness and the TUNEL assay was performed as previously described (Abuzeid *et al*, 2009). Four tumour sections were randomly selected from each treatment group and apoptotic cells were quantified and analysed using the ImageJ software (National Institutes of Health (NIH), Bethesda, MD, USA).

***In vivo* animal and xenograft tumours.** All animal handling and surgical procedures were conducted strictly according to the guiding principles for the use of laboratory animals. This study was approved by the Animal Care Committee guidelines of the University of Pennsylvania. Six-week-old female athymic BALB/c nude mice obtained from the National Cancer Institute were randomly divided into four groups with three mice each. Mice were anaesthetised via i.p. injection of 6–10 mg tribromoethanol, with depth of anaesthesia determined by toe pinch. Mice were then injected subcutaneously in the left flank with either ten million Fadu or JHU022 cells. Eight days status-post tumour injection, mice in the treatment group received 25 mg kg<sup>-1</sup> *w/v* BV twice daily *via* i.p. injection, with equivalent PBS *w/v* serving as a control. To measure BV's effect on dynamic tumour growth, every 2 days after treatment, external tumour measurements in two dimensions using calipers were performed. External tumour volume was calculated using the formula  $A^2 \times B \times \pi/6$ , where *A* represents the smallest diameter and *B* equals the largest diameter, as previously described by Roulin *et al* (2010).

**Statistical analysis.** All experiments were performed three times, and all statistical analysis including s.d./s.e.m. calculations were performed using SPSS 11.5 (Chicago, IL, USA). Differences/correlations between groups were calculated with Student's *t*-test or Mann-Whitney *U*-test, and solitary outliers (> 2 s.d.'s) were removed from analysis. A *P*-value of < 0.05 was used as a measure of statistical significance.

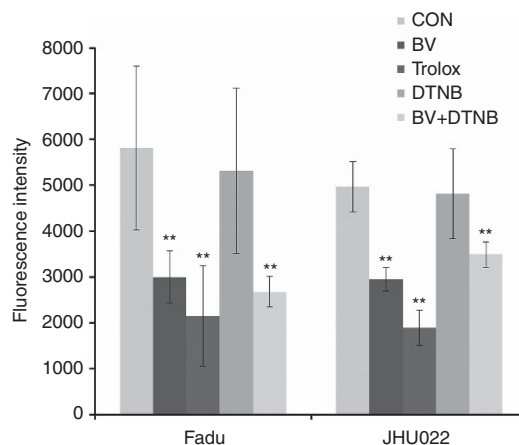


**Figure 2.** BV has a potent suppressive effect on ROS levels *in vitro*. To demonstrate the antiproliferative effect of BV, an ROS assay was performed on Fadu and JHU022 cancer cells as described earlier. In three independent experiments with at least three samples each, treatment with BV, Trolox, and BV plus DTNB significantly suppressed the ROS level in both HNSCC cells tested (\*\**P* < 0.01), while DTNB treatment alone did not change the ROS level. Mean  $\pm$  s.d. is shown.

## RESULTS

**BV suppresses colony formation *in vitro*.** To demonstrate BV's antiproliferative effect on HNSCC cells, a clonogenic assay was performed. After 3 days of treatment, both Fadu and JHU022 cells saw a striking decrease in colony forming ability of 51.59% and 47.11%, respectively ( $P < 0.01$ ), as compared with control (Figure 1). These results suggest a significant antiproliferative effect of BV on HNSCC cells.

**BV suppresses ROS *in vitro*.** To assess whether BV treatment leads to ROS suppression in tumour cells and to parse out whether this antioxidant effect is secondary to BV reductase (BVR) suppression, we investigated the ROS levels in both Fadu and JHU022 cells with or without BV, Trolox (a positive control), and DTNB (a potent BVR inhibitor). In both cell lines, treatment with BV, Trolox, or BV plus DTNB led to a significant decrease in ROS levels (Figure 2) ( $P < 0.01$ ). There was, however, no significant change in ROS after DTNB treatment ( $P > 0.05$ ), clearly

demonstrating that BV's antioxidant effect is independent of its conversion to BR by BVR.

**BV suppresses ROS-mediated expression and phosphorylation of EGFR, HIF1- $\alpha$ , Akt, and cell-cycle proteins.** To further characterise the pathways governing this antiproliferative effect of BV, we first looked to assess whether treatment with BV antiproliferative effect is due to inhibition of growth pathways, specifically EGFR signalling. Biliverdin, Trolox, and BV plus DTNB resulted in a significant decrease in the expression of both EGFR and p-EGFR in Fadu and JHU022 cells (Figure 3A). Similarly, BV, Trolox, and BV plus DTNB led to a significant downregulation of p-Akt in Fadu and JHU022 cells (Figure 3A). We also wanted to evaluate whether BV had an inhibitory effect on ROS-mediated angiogenic pathways, namely through expression of HIF1- $\alpha$ . Biliverdin, Trolox, and BV plus DTNB led to a significant downregulation of HIF1- $\alpha$  expression in both tested cell lines (Figure 3B). Finally, we also looked to evaluate whether this ROS inhibitory effect led to inhibition of ROS-dependent cell-cycle progression. Our results demonstrate that p-Rb and Cyclin D1,

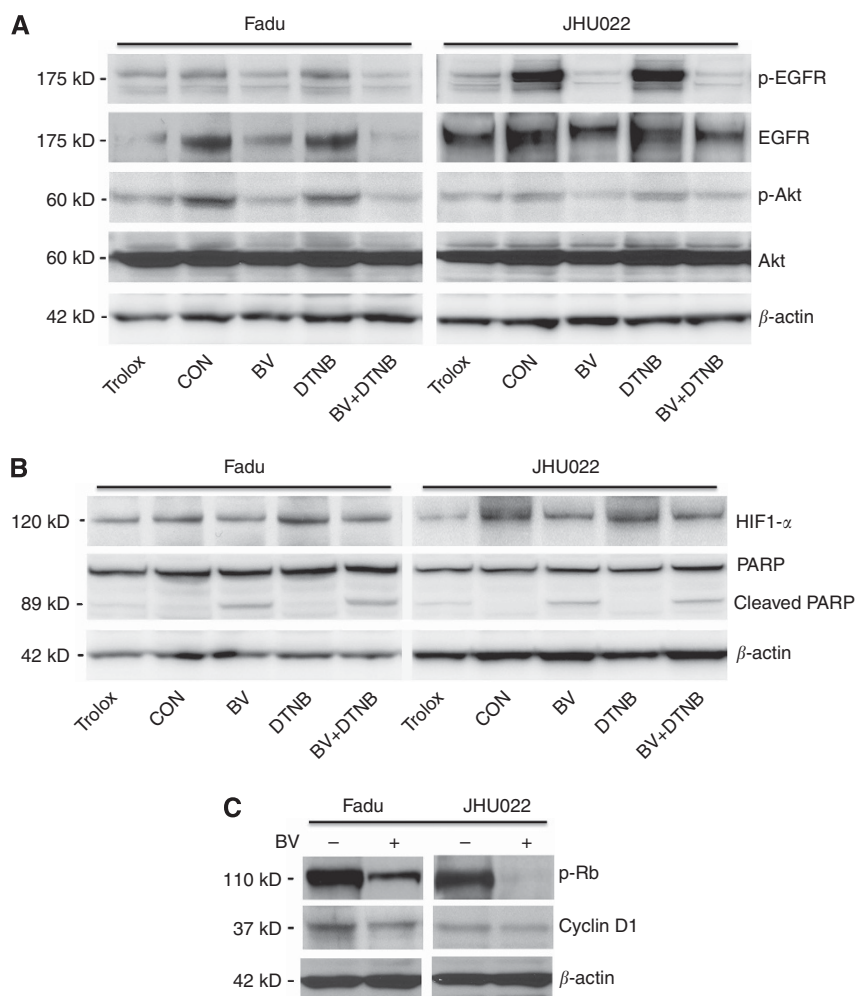


**Figure 3.** BV suppresses both the expression and phosphorylation of EGFR, and the phosphorylation of Akt. Western blot analysis was conducted on Fadu and JHU022 cell lines assessing expression and phosphorylation of EGFR and Akt. In both cell lines, BV, Trolox, and BV plus DTNB decreased expression of EGFR, p-EGFR, and p-Akt (A). We also evaluated BV's effect on ROS-mediated expression of HIF1- $\alpha$ . In both cell lines, BV, Trolox, and BV plus DTNB led to a significant downregulation of HIF1- $\alpha$  expression (B), while DTNB alone had no effect. We also evaluated whether BV led to inhibition of ROS-mediated cell-cycle progression by looking at the effect of BV treatment on p-Rb 807/811 and cyclin D1. In both cell lines, BV treatment significantly decreased p-Rb and cyclin D1 expression, as compared with control (C). Finally, to characterise whether the antiproliferative, antiangiogenic, and anti-cell cycle progression effect of BV leads to an increase in apoptosis, we evaluated cleaved PARP expression. In both cell lines, BV, Trolox, and BV plus DTNB groups saw increased cleavage of PARP, while DTNB treatment alone exhibited no effect (B).  $\beta$ -Actin was used as a loading control in all experiments. All groups were evaluated 72 h after treatment.

both critical mediators of cell-cycle progression, had significantly decreased expression in both cell lines when treated with BV (Figure 3C).

Previously, it has been established that inhibition of growth factor signalling, angiogenesis, and cell cycle is associated with increased apoptosis (Ollinger *et al*, 2007a). To determine whether the inhibition of these pathways using BV leads to increased apoptotic mechanisms, we evaluated the expression of cleaved PARP after BV, Trolox, and BV plus DTNB treatment. Seventy-two hours after treatment with BV, Trolox, or BV plus DTNB, both

Fadu and JHU022 cells showed a significant increase in PARP cleavage. Similar to our other findings, DTNB treatment alone did not affect PARP cleavage (Figure 3B).

**BV targets angiogenesis pathways and inhibits tumour growth *in vivo*.** To further assess the antitumour effect of BV, our mouse model with HNSCC was used to evaluate tumour growth. Tumour size was assessed every 2 days after BV treatment (Figure 4A and B). In both groups, mice treated with BV were found to have a significant decrease in tumour growth, with antitumour effects

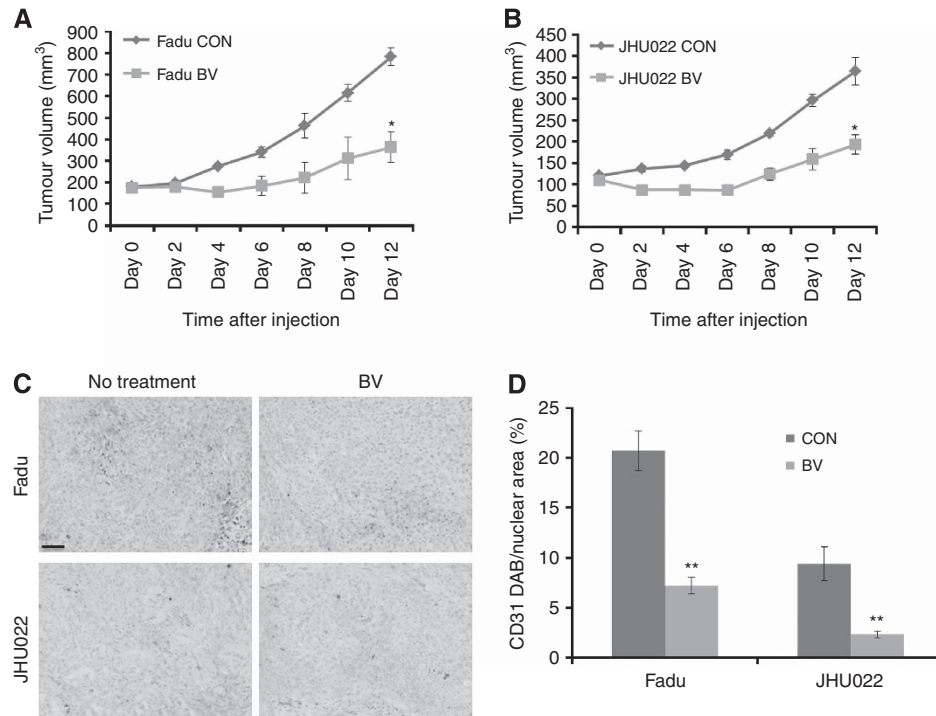


**Figure 4.** BV inhibits Fadu and JHU022 tumour growth *in vivo* and angiogenetic pathway. BV treatment at  $25 \text{ mg kg}^{-1}$  twice daily dramatically reduced Fadu (A) and JHU022 (B) tumour growth *in vivo* start from day 4 in Fadu xenograft (from day 2 in JHU022 xenograft),  $**P < 0.05$ . Results are representative of three times measurement and mean of relative volume change  $\pm$  s.e.m. is shown. (C) BV inhibits Fadu and JHU022 xenograft angiogenesis *in vivo*, with (D) representing the quantification of (C). BV induced a 2.9-fold decrease in CD31 expression of Fadu cells (20.70%;  $**P < 0.01$ ) and a 4.1-fold decrease in JHU022 cells (9.40%;  $**P < 0.01$ ) relative to control groups. Scale bar,  $50 \mu\text{m}$ .

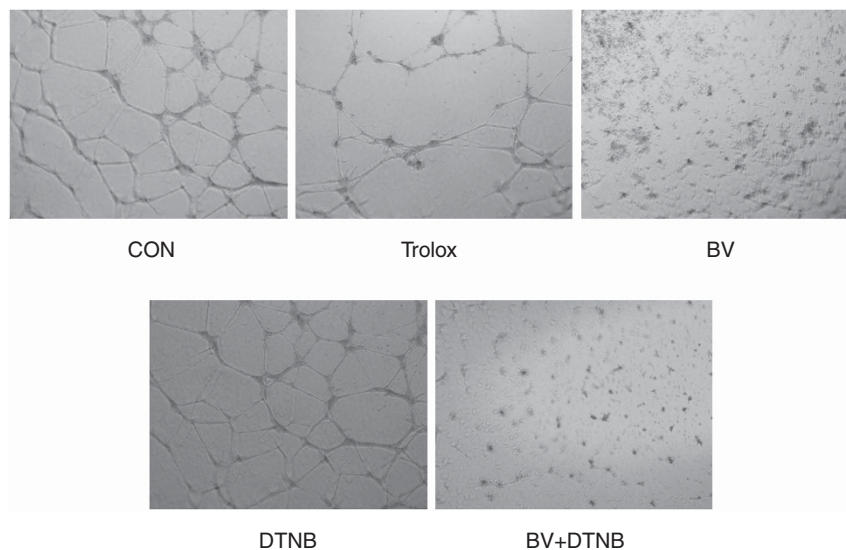


**Figure 5.** BV decreases HUVECs tube formation *in vitro*. Our findings further confirm that as compared with control, where HUVECs form robust tube structures, BV, Trolox, and BV plus DTNB inhibit the formation of these structures, while DTNB alone has no effect.

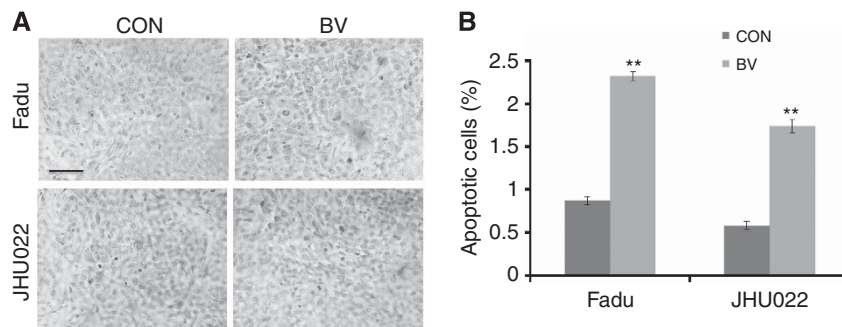


**Figure 6.** BV increases Fadu and JHU022 tumour apoptosis *in vivo*. BV treatment at  $25 \text{ mg kg}^{-1}$  twice daily dramatically increased Fadu (A) and JHU022 (B); BV induced a 2.6-fold increase in apoptotic response of Fadu cells (2.32%;  $P < 0.01$ ) and a 3.1-fold increase in JHU022 cells (1.77%;  $**P < 0.01$ ) relative to control groups. Scale bar,  $50 \mu\text{m}$ .

appearing as early as day 2 and remaining sustained through day 12 (Fadu:  $P = 0.038$ ; JHU022:  $P = 0.039$ ). In addition, by day 12, mice treated with BV detected a reduction in tumour volume by 64.76% ( $P < 0.05$ ) for Fadu and 91.59% ( $P < 0.05$ ) for JHU022, as compared with control. Furthermore, the effect of BV on *in vivo* angiogenesis was also evaluated, showing a significant down-regulation of angiogenesis, as measured by MVD of CD31. Tumours treated with BV demonstrated significant antiangiogenic effects in both cell lines (Figure 4C and D). These dramatic *in vivo* findings further confirm that BV is an effective antitumour agent, which has the potential to serve as a novel natural molecular inhibitor for HNSCC.

**BV suppresses HUVECs tube formation *in vitro*.** To better understand whether the antiangiogenic effect of BV is secondary to its inhibition of ROS, we conducted the Matrigel tube formation assay *in vitro* with HUVECs treated with BV, Trolox, DTNB, or BV plus DTNB for 3 days. In comparison with the control group where robust tube structures were found, BV, Trolox, and BV plus DTNB treatments led to a significant inhibition in HUVEC tube formation, but DTNB alone had no effect (Figure 5).

**BV promotes tumour apoptosis *in vivo*.** To confirm whether the antiproliferation and antiangiogenic effect of BV leads to increased apoptosis *in vivo*, a TUNEL assay was performed. Biliverdin treatment dramatically increased tumour apoptosis *in vivo* (Figure 6A), inducing a 2.6-fold increase in apoptotic response of Fadu group (2.32%;  $P < 0.01$ ) and a 3.1-fold increase in JHU022 group (1.77%;  $P < 0.01$ ) relative to control groups (Figure 6B).

## DISCUSSION

This study set out to evaluate whether BV treatment led to an inhibitory effect on HNSCC cells, and explored the mechanism underlying our findings. Our results demonstrate that BV treatment, independent of BR, decreases ROS activity in the cell, leading to decreased EGFR, HIF1- $\alpha$ , and cell-cycle protein expression and activity subsequently leading to a significant inhibition of downstream tumour growth and angiogenesis pathways, respectively. Furthermore, our results fill gaps in current mechanistic understanding of previously reported clinical correlations between serum BR levels and tumour incidence, while clearly demonstrating the use of BV as an effective treatment modality. *In vitro*, BV inhibited proliferative capacity of various HNSCC cell lines. The antiproliferative effects seen were a consequence of the interruption of the EGFR/Akt signalling pathway and cell-cycle progression, leading to induction of the intrinsic apoptotic response. Before our study, others have reported that the BR may alter proliferation of cancer cells, but were unable to effectively demonstrate the mechanism underlying this finding.

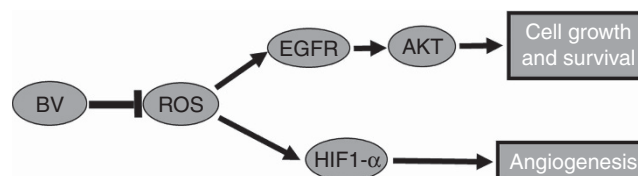


**Figure 7.** Signalling pathways involved in BV-mediated growth suppression and angiogenesis induction in HNSCC cells. BV via ROS suppresses EGFR/Akt and HIF1- $\alpha$  subsequently suppresses cell growth and survival and angiogenesis.

Biliverdin, a non-toxic homologue of toxic BR, therefore, serves as a better clinical correlate to this therapeutic approach. Therefore, in this study we looked to identify the underlying mechanism for the effect of BV treatment on HNSCC cells, focussing our study on the effect of BV on proliferative, cell cycle, angiogenesis, and apoptotic pathways.

Upregulation of EGFR expression and signalling have been associated with numerous cancers, including lung cancer, breast cancer, and HNSCC. Increased activation of EGFR through its tyrosine kinase activity has been shown to initiate signal transduction cascades, principally through the Akt pathway, leading to increased DNA synthesis, cellular proliferation, and tumour progression. Moreover, ROS has been shown to be an important regulator of EGFR expression, activity, and downstream signalling pathways. Therefore, in light of BV's potent inhibition of cancer cell growth and previously reported antioxidant effect, we looked to evaluate the effect of BV on this ROS-mediated EGFR signalling pathway. Biliverdin treatment resulted in a profound downregulation of ROS, independent of its conversion to BR by BVR, leading to suppression of both EGFR expression and phosphorylation. Furthermore, this decrease in phosphorylation led to decreased downstream signalling as evidenced by decreased Akt phosphorylation. Furthermore, we also demonstrated that BV treatment leads to a downregulation of p-Rb and cyclin D1, essential components of the cell-cycle progression machinery also regulated by ROS. We also demonstrated that BV leads to a downregulation of ROS-mediated HIF1- $\alpha$ , leading to decreased angiogenesis *in vivo*, and providing a significant leap in the current understanding of angiogenic pathways hinging on haeme oxygenase activity and carbon monoxide. Biliverdin's feedback inhibition of this angiogenic pathway provides a salient basis for not only this study, but others focussing on the specific factors involved in this pathway. To demonstrate that these effects are directly resulting from primarily BV's antioxidant effect and not a secondary effect from BR, we used a potent antioxidant as a positive control and a BVR inhibitor to block BV's conversion to BR. Our results clearly demonstrate that Trolox, the antioxidant, mirrors BV's effect on

EGFR, Akt, HIF1- $\alpha$ , p-Rb, and Cyclin D1 expression and has a similar effect on apoptosis and angiogenesis pathways, while DNTB, the BVR inhibitor (Supplementary Figure S1), had no significant effect. While there is still an effect of BV in the presence of DNTB, suggesting that the antiproliferative and antiangiogenesis effects do not rely on BR generation, DNTB may have other non-specific pharmacologic effects in the cell, which is a potential limitation of our findings. Future study using other more specific molecular approaches might be warranted to further clarify this pathway.

While our *in vitro* results provide a strong basis for this study, we wanted to confirm our findings using a robust *in vivo* HNSCC tumour model. Herein, we found BV to be a very effective antitumour agent, with a significant decrease in tumour growth seen as early as day 2 post treatment. Furthermore, we demonstrate that it achieves this goal without significant toxic effects on the mice, demonstrated by lack of changes in weight loss, post-treatment survival (Supplementary Figure S2), and liver dysfunction (Supplementary Figure S3). To our knowledge, this is the first study to describe BV's antiproliferative effect in an animal model, therefore providing some evidence for its translational applicability.

In summary, we demonstrate that BV is a potent, naturally occurring, antitumour agent that mediates growth inhibition of HNSCC cells through induction of antiproliferative, pro-apoptotic, and antiangiogenic pathways (Figure 7). This study demonstrates that BV potently suppresses tumour growth, a phenomenon that may in part explain the observed negative clinical correlation between cancer incidence and serum BR levels. Moreover, this study provides the basis for evaluating the use of non-toxic BV to other cancers that rely on ROS for intracellular signalling.

## REFERENCES

- Abuzeid WM, Jiang X, Shi G, Wang H, Paulson D, Araki K, Jungreis D, Carney J, O'Malley Jr BW, Li D (2009) Molecular disruption of RAD50 sensitizes human tumor cells to cisplatin-based chemotherapy. *J Clin Invest* **119**(7): 1974–1985.
- Ahluwalia A, Tarnawski AS (2012) Critical role of hypoxia sensor-HIF-1 $\alpha$  in VEGF gene activation. Implications for angiogenesis and tissue injury healing. *Curr Med Chem* **19**(1): 90–97.
- Arnautova I, George J, Kleinman HK, Benton G (2009) The endothelial cell tube formation assay on basement membrane turns 20: state of the science and the art. *Angiogenesis* **12**(3): 267–274.
- Asad SF, Singh S, Ahmad A, Khan NU, Hadi SM (2001) Prooxidant and antioxidant activities of bilirubin and its metabolic precursor biliverdin: a structure-activity study. *Chem Biol Interact* **137**(1): 59–74.
- Ching S, Ingram D, Hahnel R, Beilby J, Rossi E (2002) Serum levels of micronutrients, antioxidants and total antioxidant status predict risk of breast cancer in a case control study. *J Nutr* **132**(2): 303–306.
- Choi KS, Bae MK, Jeong JW, Moon HE, Kim KW (2003) Hypoxia-induced angiogenesis during carcinogenesis. *J Biochem Mol Biol* **36**(1): 120–127.
- Dobashi Y, Suzuki S, Kimura M, Matsubara H, Tsubochi H, Imoto I, Ooi A (2011) Paradigm of kinase-driven pathway downstream of epidermal growth factor receptor/Akt in human lung carcinomas. *Hum Pathol* **42**(2): 214–226.
- Dortay H, Akula UM, Westphal C, Sittig M, Mueller-Roeber B (2011) High-throughput protein expression using a combination of ligation-independent cloning (LIC) and infrared fluorescent protein (IFP) detection. *PLoS One* **6**(4): e18900.
- Dudek H, Datta SR, Franke TF, Birnbaum MJ, Yao R, Cooper GM, Segal RA, Kaplan DR, Greenberg ME (1997) Regulation of neuronal survival by the serine-threonine protein kinase Akt. *Science* **275**(5300): 661–665.
- Fondevila C, Shen XD, Tsuchiyashi S, Yamashita K, Csizmadia E, Lassman C, Busuttill RW, Kupiec-Weglinski JW, Bach FH (2004) Biliverdin therapy protects rat livers from ischemia and reperfusion injury. *Hepatology* **40**(6): 1333–1341.
- Leemans CR, Braakhuis BJ, Brakenhoff RH (2011) The molecular biology of head and neck cancer. *Nat Rev Cancer* **11**(1): 9–22.
- Li D, Guang W, Abuzeid WM, Roy S, Gao GP, Sauk JJ, O'Malley Jr BW (2008) Novel adenoviral gene delivery system targeted against head and neck cancer. *Laryngoscope* **118**(4): 650–658.
- Liu Y, Zhu B, Wang X, Luo L, Li P, Paty DW, Cynader MS (2003) Bilirubin as a potent antioxidant suppresses experimental autoimmune encephalomyelitis: implications for the role of oxidative stress in the development of multiple sclerosis. *J Neuroimmunol* **139**(1–2): 27–35.
- MacLean PD, Chapman EE, Dobrowolski SL, Thompson A, Barclay LR (2008) Pyrroles as antioxidants: solvent effects and the nature of the attacking radical on antioxidant activities and mechanisms of pyrroles, dipyrinones, and bile pigments. *J Org Chem* **73**(17): 6623–6635.
- Mavria G, Harrington KJ, Marshall CJ, Porter CD (2005) In vivo efficacy of HSV-TK transcriptionally targeted to the tumour vasculature is augmented by combination with cytotoxic chemotherapy. *J Gene Med* **7**(3): 263–275.
- Molzer C, Huber H, Steyrer A, Ziesel G, Ertl A, Plavotic A, Wallner M, Bulmer AC, Wagner KH (2012) In vitro antioxidant capacity and antigenotoxic properties of protoporphyrin and structurally related tetrapyrroles. *Free Radic Res* **46**(11): 1369–1377.
- Mosqueda L, Burnight K, Liao S (2005) The life cycle of bruises in older adults. *J Am Geriatr Soc* **53**(8): 1339–1343.
- Ollinger R, Bilban M, Erat A, Froio A, McDaid J, Tyagi S, Csizmadia E, Graca-Souza AV, Liloia A, Soares MP, Otterbein LE, Usheva A, Yamashita K, Bach FH (2005) Bilirubin: a natural inhibitor of vascular smooth muscle cell proliferation. *Circulation* **112**(7): 1030–1039.
- Ollinger R, Kogler P, Troppmair J, Hermann M, Wurm M, Drasche A, Konigsrainer I, Amberger A, Weiss H, Ofner D, Bach FH, Margreiter R (2007a) Bilirubin inhibits tumor cell growth via activation of ERK. *Cell Cycle* **6**(24): 3078–3085.
- Ollinger R, Yamashita K, Bilban M, Erat A, Kogler P, Thomas M, Csizmadia E, Usheva A, Margreiter R, Bach FH (2007b) Bilirubin and biliverdin treatment of atherosclerotic diseases. *Cell Cycle* **6**(1): 39–43.
- Roulin D, Cerantola Y, Dormond-Meuwly A, Demartines N, Dormond O (2010) Targeting mTORC2 inhibits colon cancer cell proliferation in vitro and tumor formation in vivo. *Mol Cancer* **9**: 57.
- Saito K, Khan K, Sosnowski B, Li D, O'Malley Jr BW (2009) Cytotoxicity and antiangiogenesis by fibroblast growth factor 2-targeted Ad-TK cancer gene therapy. *Laryngoscope* **119**(4): 665–674.
- Sarady-Andrews JK, Liu F, Gallo D, Nakao A, Overhaus M, Ollinger R, Choi AM, Otterbein LE (2005) Biliverdin administration protects against endotoxin-induced acute lung injury in rats. *Am J Physiol Lung Cell Mol Physiol* **289**(6): L1131–L1137.
- Stocker R (2004) Antioxidant activities of bile pigments. *Antioxid Redox Signal* **6**(5): 841–849.
- Temme EH, Zhang J, Schouten EG, Kesteloot H (2001) Serum bilirubin and 10-year mortality risk in a Belgian population. *Cancer Causes Control* **12**(10): 887–894.
- Tuominen VJ, Ruotoistenmaki S, Viitanen A, Jumppanen M, Isola J (2010) ImmunoRatio: a publicly available web application for quantitative image analysis of estrogen receptor (ER), progesterone receptor (PR), and Ki-67. *Breast Cancer Res* **12**(4): R56.
- Turcanu V, Dhouib M, Poindron P (1998) Determination of heme oxygenase activity in murine macrophages for studying oxidative stress inhibitors. *Anal Biochem* **263**(2): 251–253.
- Yamashita K, McDaid J, Ollinger R, Tsui TY, Berberat PO, Usheva A, Csizmadia E, Smith RN, Soares MP, Bach FH (2004) Biliverdin, a natural product of heme catabolism, induces tolerance to cardiac allografts. *FASEB J* **18**(6): 765–767.
- Zucker SD, Horn PS, Sherman KE (2004) Serum bilirubin levels in the U.S. population: gender effect and inverse correlation with colorectal cancer. *Hepatology* **40**(4): 827–835.

This work is published under the standard license to publish agreement. After 12 months the work will become freely available and the license terms will switch to a Creative Commons Attribution-NonCommercial-Share Alike 3.0 Unported License.